FR8002096

Wire chamber conference.
Vienna, Austria, february 27 - 29, 1980.
CEA - CONF 5224

MULTI-STEP AVALANCHE CHAMBERS FOR FNAL EXPERIMENT E605

J.R. Hubbard, G. Coutrakon*, M. Cribier, Ph. Mangeot,
H. Martin, J. Mullié, S. Palanque, J. Pelle.

CEN-SACLAY, DPhPE-STIPE, BP N°2, 91190 Gif sur Yvette, France

- 1980 -

* Also at SUNY at Stony Brook, NEW-YORK (USA)

- A B S T R A C T -

Physical processes in multi-step avalanche chambers, detector properties, and difficulties in operation are discussed. Advantages of multi-step chambers over classical MWPC for specific experimental problems encountered in experiment E605 (high-flux environment and ČERENKOV imaging) are described. Some details of detector design are presented.

1 - INTRODUCTION

At SACLAY we are investigating multi-step avalanche chambers (MSAC)[1], in collaboration with CHARPAK and SAULI at CERN, to solve two specific problems for FERMILAB experiment E605[2]:

a) Detect single and double tracks in a high average flux,

b) Detect ČERENKOV radiation for ring-imaging particles with $\gamma \geq 100$.

In this paper we will discuss some properties of the MSAC, problems encountered in construction of large chambers, advantages of MSAC over classical multi-wire proportional chambers (MWPC), and design strategy for the E605 high-flux and ČERENKOV counters.

2 - MULTI-STEP AVALANCHE CHAMBER OPERATION

2-1) Amplification mechanism :

We have studied the preamplification and transfer process (PAT)[3] in various gas mixtures in an attempt to understand the mechanism and select appropriate gases.

As electrons gain energy ($\mathcal{E}$) in an electric field, they cross thresholds for several different amplification processes[4]. If the ionization potential (I_x) of the contaminating polyatomic molecule is lower than the excitation energy (E^*) of the noble gas, these thresholds are ordered as follows :

a) Direct ionization of the polyatomic molecule ($\mathcal{E} > I_x$);

b) Indirect ionization of the polyatomic molecule by an excited noble gas atom or molecule ($\mathcal{E} > E^*$);

c) Direct ionization of the noble gas ($\mathcal{E} > I_R$), the noble gas ionization potential).

Excited argon atoms can lose their energy by photon emission or by molecular collision (Penning effect)[5]. In pure argon at atmospheric pressure, most atoms degrade their energy by dimer production (formation time 0.5 μsec) before de-excitation by photoemission (decay times 3 μsec for the most populated state, 4 nsec for a less populated state)[6]. With polyatomic molecules present, the Penning effect should de-excite the argon at rates much higher than the dimer production rate[7].

We have observed the PAT mechanism with argon mixed with small amounts of the following gases :

a) Acetone, with I_x = 9.7 eV, near the peak of argon dimer emission;[8]

b) Propane, with I_x = 11.1 eV;

c) Acetylene, with I_x = 11.4 eV, just below the first excitation level of argon at 11.55 eV;

d) Methane, with I_x = 13 eV, above the metastable excitation levels of argon, but below the second resonant level at 14 eV. (Pulses obtained with argon/methane are shown in Fig.1).

We obtained similar amplification factors and transfer fractions for all these additives, suggesting that dimer de-excitation is not playing a dominant role in the PAT process. Direct ionization by electron collision (probably with the poly-atomic component) would seem to be more important).

2-2) Pulses :

An electron cloud of change Q, drifting with velocity W between two electrodes separated by a distance L produces a current of magnitude QW/L. When multiplication occurs with TOWNSEND coefficient α ,

$$\frac{dq}{dt} = - \frac{QW}{L} \; e^{\alpha W t}$$

(neglecting positive-ion movement).

After a drift time $t_1 = L/W$, all electrons have reached the second electrode (neglecting longitudinal diffusion); the charge pulse observed on this second electrode is equal to :

$$q(t_1) = - Q \left[\frac{e^{\alpha L} - 1}{\alpha L}\right] = - Q \left[\frac{G - 1}{\ln G}\right]$$

where $G = e^{\alpha L}$ is the total gain of the gap, but only a fraction $(1/\ln G)$, typically 10%, is observed as a fast pulse, due to the proximity of the positive ions.

By transferring a fraction f of the charge to a third electrode, a larger pulse equal to - fQG car be obtained. The fraction transferred is roughly equal to the ratio of the electric fields, $f \approx E_2/E_1$ for E_2 less than about 1/2 E_1 [1].

In the case of total ionization Q initially deposited uniformly in the amplification gap (PA) :

$$\frac{dq}{dt} = - \frac{QW}{L} \left(1 - \frac{Wt}{L}\right) e^{\alpha W t}$$

and

$$q(t_1) = - Q \left[\frac{G - \ln G - 1}{(\ln G)^2}\right]$$

2-3) Parallelism and uniformity :

The measured pulse height and calculated gain for a 4 mm PA gap are shown in Fig.2 as a function of the electric field (E). The Townsend coefficient $\alpha = (\ln G)/L$ is plotted in the lower figure. A straight-line approximation $\alpha = BE - k$ yields $1/B \approx 85$ Volts, $1/k \approx 130\,\mu$m for argon plus 5% propane in the region of interest ($E \geqslant 7$ kV/cm).

Any lack of parallelism in the amplification gap induces an exponential difference in gain :

$$G(L - \delta) = G(L)\, e^{k\delta}$$

We have verified this relation by measuring gains in a controlled non-parallel gap.

This non-uniformity is critical for large chambers, because of the electrostatic attraction produced by the strong field in the PA gap. The displacement is parabolic (for wire planes) with a maximum :

$$d \approx \frac{\varepsilon_0\, sE^2 \ell^2}{8T}$$

for wire spacing s, length ℓ, and wire tension T. (For fields E_1 and E_2 inside and outside the gap, $E^2 \rightarrow E_1^2 - E_2^2$. For grids, $\ell^2 \rightarrow (\ell_1^{-2} + \ell_2^{-2})^{-1}$).

We have tested a large PA gap (60 x 90 cm^2, L = 2.8 mm) for uniformity of response. The results are displayed in Fig.3. Using the value $1/k = 130\,\mu$m, we find $2d = 1.3$ mm, consistent with displacements measured on the individual grids before assembly. The range of gains is thus $G_{max}/G_{min} = e^{2kd} \approx 20\,000$.

The problem of electrostatic attraction can be greatly alleviated by placing supports between the two electrodes. For wires, N supports reduce the ratio G_{max}/G_{min} to its $(N+1)^2$ root! For our grids, two supports should reduce G_{max}/G_{min} to about 5. Tests are currently underway with accurately-machined supports and increased tension to obtain reasonable ($\pm$25%) uniformity of gain.

2-4) Gas mixture :

At constant voltage, in argon/acetone mixtures, we have observed gain variations proportional to the tenth power of the acetone partial pressure (P_x): $G \sim 1/P_x^{10}$. This rapid variation results from the fact that the argon cross section is small and elastic for electron energies below the first excitation level; the noble gas serves mainly to separate the polyatomic gas molecules. In fact, amplification in pure polyatomic gases at low pressure is used in the parallel plate avalanche counter (PPAC) [9].

In any case, the strong gain variations with P_x add to the difficulty of obtaining stable MSAC operation. A gas monitor will be required to control chamber voltages.

2-5) Time jitter :

Three contributions to time jitter in a MSAC should be mentioned :

a) Jitter in the location of the primary ionization;

b) Dynamic range of the pulses (LANDAU-type distribution coupled with spatial variation of the gain;

c) Longitudinal diffusion of the electrons.

For 98% detection efficiency, four ionization lengths must be included, giving a minimum time jitter in argon of (1.2 mm x 20 nsec/mm) = 24 nsec in fast gas mixtures.

Experimentally (see CHARPAK's talk)[10] time jitters of about 15 nsec FWHM and 90 nsec (full efficiency) are observed. With a 30 nsec electrostatic gate these times can be reduced to 10 nsec FWHM and 60 nsec at the base. But much longer occupation times of some 80 to 100 nsec were observed.

2-6) MSAC summary :

We have insisted on two difficulties of large MSAC: gain non-uniformity due to small parallelism defects and extreme sensitivity to the partial pressure of the polyatomic gas components. Another difficulty is their remarkable propensity for sparking.

Long drift distances (typically $\sim$ 25 mm) render the MSAC like drift chambers, but unlike MWPC, sensitive to magnetic fields.

Timing considerations, originally thought to favor the MSAC over the MWPC are, in fact, similar for the two types of detector.

Spatial resolution on anode wires can be made finer for MSAC, first because the wires are more closely spaced (0.5 mm), and further because the electron cloud induces signals on more than one wire, so interpolation is possible[1]. Good resolution can be obtained for multiple coordinates (with correlated amplitudes) by adding successive read-out planes after the second amplification gap.

Two major advantages of the MSAC account for the interest for E605 :

1) A high -flux capability made possible by separating the two amplification gaps by an electrostatic gate ;

2) Good (100%) single-electron detection efficiency required for ČERENKOV ring-imaging[11].

3 - FNAL EXPERIMENT E605

FERMILAB experiment E605 is designed to study particle pairs and single tracks at large transverse momentum, near the kinematic limit[2]. The experimental group includes FNAL, COLUMBIA, STONY BROOK and SEATTLE in the U.S.A.; KEK, KYOTO and TOKYO in Japan; and CERN and SACLAY in Europe for the multistep chambers.

A 15 meter magnet (M12) with bevelled aluminium coils produces 30 kG at the magnet entrance and 15 kG at the exit, and delivers a 10 GeV/c momentum kick. Both transverse momentum and the mass of pairs are measured extremely accurately (0.1%).

The experiment should begin in the second half of 1981 at 400 GeV/c with 3×10^{12} incident protons/burst and 10^{12} target interactions; the remaining beam is eliminated in a beam dump within the M12 magnet. The experiment will continue at TEVATRON energies.

The detector system consists of MWPC at station 1, 5 m from the M12 exit, and drift chambers at stations 2 and 3, further downstream.

3-1) High-flux station zero :

We are designing an MSAC for station zero, as close to the M12 exit as possible ($\sim$1 m) to improve background rejection. The expected average flux is about $10^8/m^2/sec$, with some regions seeing $10^4/mm^2/sec$, close to the limit for stable MWPC operation[1].

Figure 4 shows a possible design for a 100 x 130 cm^2 station zero MSAC detector. The active volume is closed by a thin (10μm) aluminum foil which forms the first electrode of a conversion space (C). The conversion space should be about four ionization lengths thick (1.2 mm of argon). The preamplification gap (PA1) should be as thin as possible (3 mm) to obtain a sharp fall-off in gain and thus minimize chamber occupation time.

The transfer gap (T1) sets the delay for the trigger. For E605, some 300 nsec are required, so PA1 plus T1 must be at least 15 mm long so that fast gas mixtures (such as argon/acetone) can be used. All other gaps should be as small as possible to minimize the total ionization in the second amplification gap (PA2).

The electrostatic gate shown here consists of wires maintained alternatively above and below the nominal voltage to keep the gate closed, and pulsed to the same potential to open it. Alternatively, the gate could use two planes, with wires in the first plane being pulsed together. Hodoscopes in the non-bend plane at stations 1 and 3 allow selective triggering on three 2-cm strips per track, out of a total width of 100 cm.

The read-out gaps (X, U, V) should be narrow (perhaps 3.2 mm) to minimize the rise time on the linear pulses. (Only the X plane is forseen in the initial design).

In light of the MSAC non-uniformities discussed in section 2, a more conservative station zero design would replace the conversion gap (C) and the narrow PA1 by a 5 mm PA1, and PA2 and the read-out gap by a MWPC operating at low amplification in the proportional mode.

3-2) Imaging ČERENKOV :

The radiator for the imaging ČERENKOV is 10 m of helium at atmospheric pressure, with sixteen 20-meter radius mirror elements focussing onto four separate MSAC detectors situated in the entrance plane near the axis. The radiator and mirrors are being designed by Robert McCARTHY and co-workers at STONY BROOK.

The current detector design, based on the best results obtained to date by CHARPAK, YPSILANTIS and co-workers[13], is shown in Fig.5. The chamber must be equipped with a very expensive mosaic of CaF_2 windows and filled with argon plus photosensitive TEA vapor (I_x = 7.5 eV). Unambiguous ring images have been obtained using a spark chamber with videcon read-out[14].

The average number of detected photoelectrons is about five for the above design. The limit on π/K separation from separation from chromatic aberrations is 10σ at 200 GeV/c and 3σ at 400 GeV/c.

4 - CONCLUSIONS

Although the MSAC are not a panacea for detection problems, they do offer new solutions for specific experimental situations. For experiment E605, the MSAC gating feature offers an important improvement in signal to noise at high-flux station zero and the good single-electron efficiency, combined with newly-developed photo-detection methods, provides the possibility of ČERENKOV ring imaging in the difficult region of $\gamma^2 \gtrsim 100$.

Acknowledgements

This work has relied heavily on help from George CHARPAK and Fabio SAULI for the multi-step chambers, Tom YPSILANTIS and Georges COMBY for ČERENKOV imaging problems, and Bob McCARTHY for all aspects of E605. We appreciate the support and encouragement of Pierre LEHMANN and Pierre PRUGNE at SACLAY.

- REFERENCES -

(1) A. BRESKIN, G. CHARPAK, S. MAJEWSKI, G. MELCHART, G. PETERSEN and F. SAULI -
Nucl. Instr. and Meth. 161 (1979) 19.

(2) L.M. LEDERMAN et al. -
"Study of Leptons and Hadrons near the kinematic limits, Addendum to Proposal 605" - (November 1978).
COLUMBIA-FERMILAB-STONY BROOK Collaboration -
"A study of 15-20 GeV massive muon pairs" - (May 1978).

(3) G. CHARPAK and F. SAULI -
Phys. Letters 78B (1978), 523.

(4) See, for example, L.G. CHRISTOPHOROU -
Atomic and Molecular Radiation Physics, Wiley-Interscience (1971).

(5) W.P. JESSE and J. SADAUSKIS -
Phys. Rev. 100 (1955), 1755.
V. ČERMÁK -
J. Chem. Phys. 44 (1966), 1318.

(6) J.W. KETO, R.E. GLEASON Jr., and G.K. WALTERS -
Phys. Rev. Lett. 33 (1974), 1365.

(7) S. KUBOTA, T. TAKAHASHI and T. DOKE -
Phys. Rev. 165 (1968), 225.

(8) Y. TANAKA -
J. Opt. Soc. Amer. 45 (1955), 710.
M. SUZUKI and S. KUBOTA -
"Mechanism of proportional scintillation in Argon, Krypton and Xenon" -
(Unpublished).

(9) H. STELZER -
Nucl. Instr. and Meth. 133 (1976), 409.
A. BRESKIN and N. ZWANG -
Nucl. Instr. and Meth. 144 (1977), 609.

(10) G. CHARPAK -
This conference.

(11) J. SEGUINOT and T. YPSILANTIS -
Nucl. Instr. and Meth. 142 (1977), 377.

(12) P. LE DÛ, P. BORGEAUD, G. BURGUN, R. HAMMARSTRÖM, R. LORENZI and A. MICHELINI -
CERN/EP, Internal report 77-11 (1977).
G. CHARPAK, F. SAULI and R. KAHN -
Nucl. Instr. and Meth. 152 (1978), 185.

(13) G. CHARPAK, S. MAJEWSKI, G. MELCHART, F. SAULI and T. YPSILANTIS -
Nucl. Instr. and Meth. 164 (1979), 419.

(14) M. VASCON and G. ZANELLA -
"Automatic scanning of ČERENKOV light photograms from multi-step avalanche chamber using a television digitizer" -
(Unpublished).

- FIGURE CAPTIONS -

Fig.1 - Pulses observed with 96% argon, 4% methane. The time scale is 1 μsec/division.
After pulses are seen in the second stage MWPC every 1500 nsec, because the gas is transparent to photons from argon de-excitation. These photons come back to the conversion gap and release new pulses of electrons from a graphited-mylar electrode. Pulses in PA1 are proportional to energy, but not those in the MWPC.

Fig.2 - Pulse height and gain in a 4 mm PA gap with 95% argon, 5% propane. The TOWNSEND coefficients for this gas mixture is shown in the lower figure, with the higher-field values approximated by a straight line $\alpha = BE - k$.

Fig.3 - Gain variations observed with a 60 x 90 cm^2 PA gap with L = 2.8 mm. The gain (G) and the distance from the center of the chamber (x) are plotted linearly in the upper figure. In the lower figure, the data are fit to the form $G = G_{max} \exp(-8kdx^2/L^2)$ appropriate to a parabolic electrostatic displacement of each PA grid. The straight line gives $2kd = 10$, so $G_{max}/G_{min} = 20\,000$.

Fig.4 - Station zero MSAC design with a thin conversion gap (C), two amplification gaps (PA1 and PA2), an electrostatic gate, and three readout planes (X, U, V). The remaining gaps (T1 and T2) are for transfer.

Fig.5 - MSAC detector for ČERENKOV ring images. U.V. ČERENKOV radiation enters the detector through a CaF_2 window and photoionizes the TEA vapor in the argon/TEA gas mixture. The photoelectrons are immediately amplified in the PA gap (PA1). After transfer and selection by the gate, the images are recorded in a spark chamber with videcon read out.

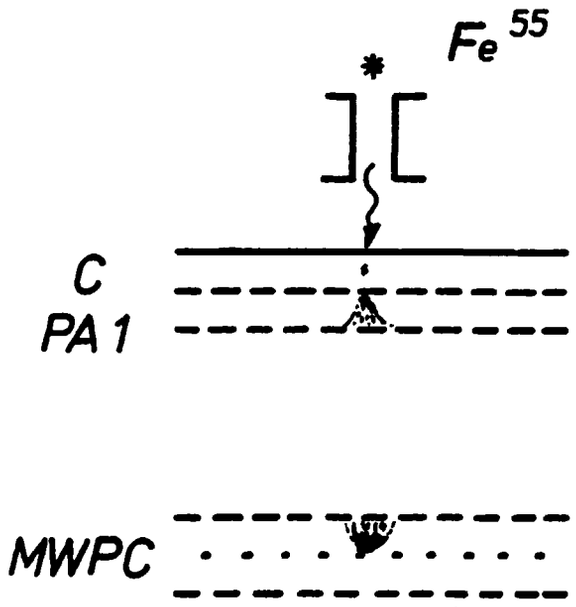

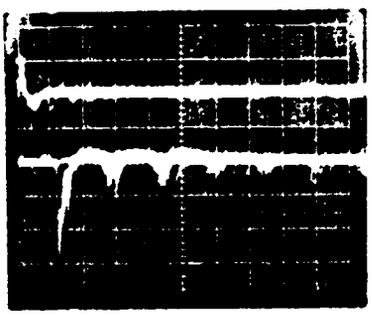

Fig: 1

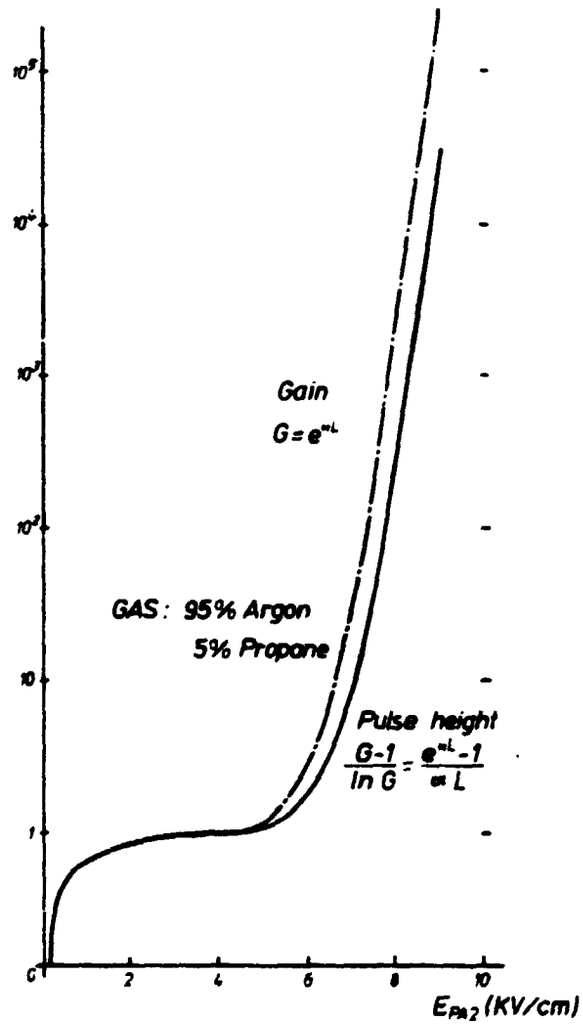
Gain
$G = e^{\alpha L}$
GAS: 95% Argon
5% Propane
Pulse height
$\frac{G-1}{\ln G} = \frac{e^{\alpha L}-1}{\alpha L}$
E_{Pk2} (KV/cm)

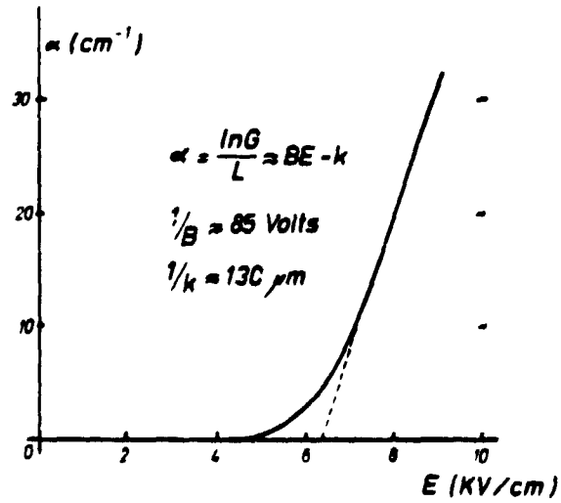
α (cm^{-1})
$\alpha = \frac{\ln G}{L} \approx BE - k$
$1/B \approx 85$ Volts
$1/k \approx 130$ μm
E (KV/cm)

Fig : 2

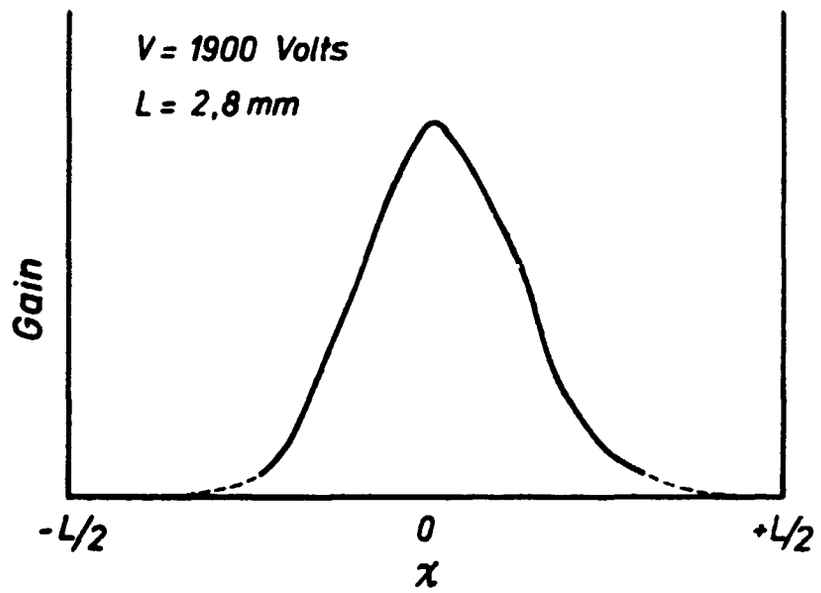
V = 1900 Volts
L = 2,8 mm
Gain
-L/2
0
+L/2
x

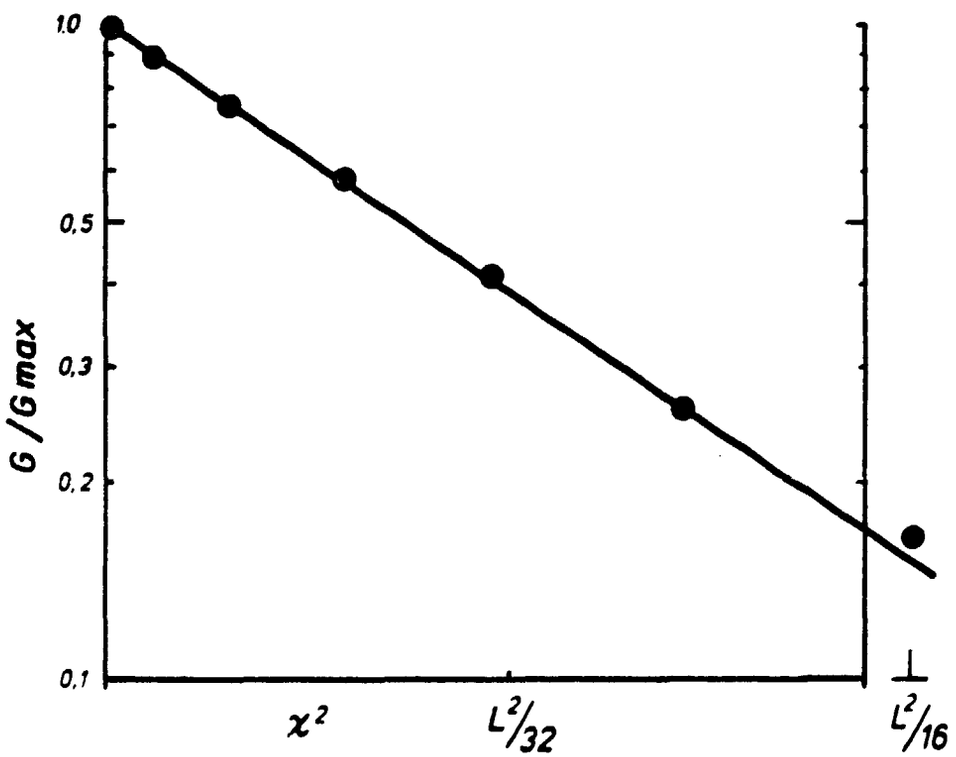
1.0
0,5
0,3
0,2
0,1
G /G max
x²
L²/32
L²/16

Fig: 3

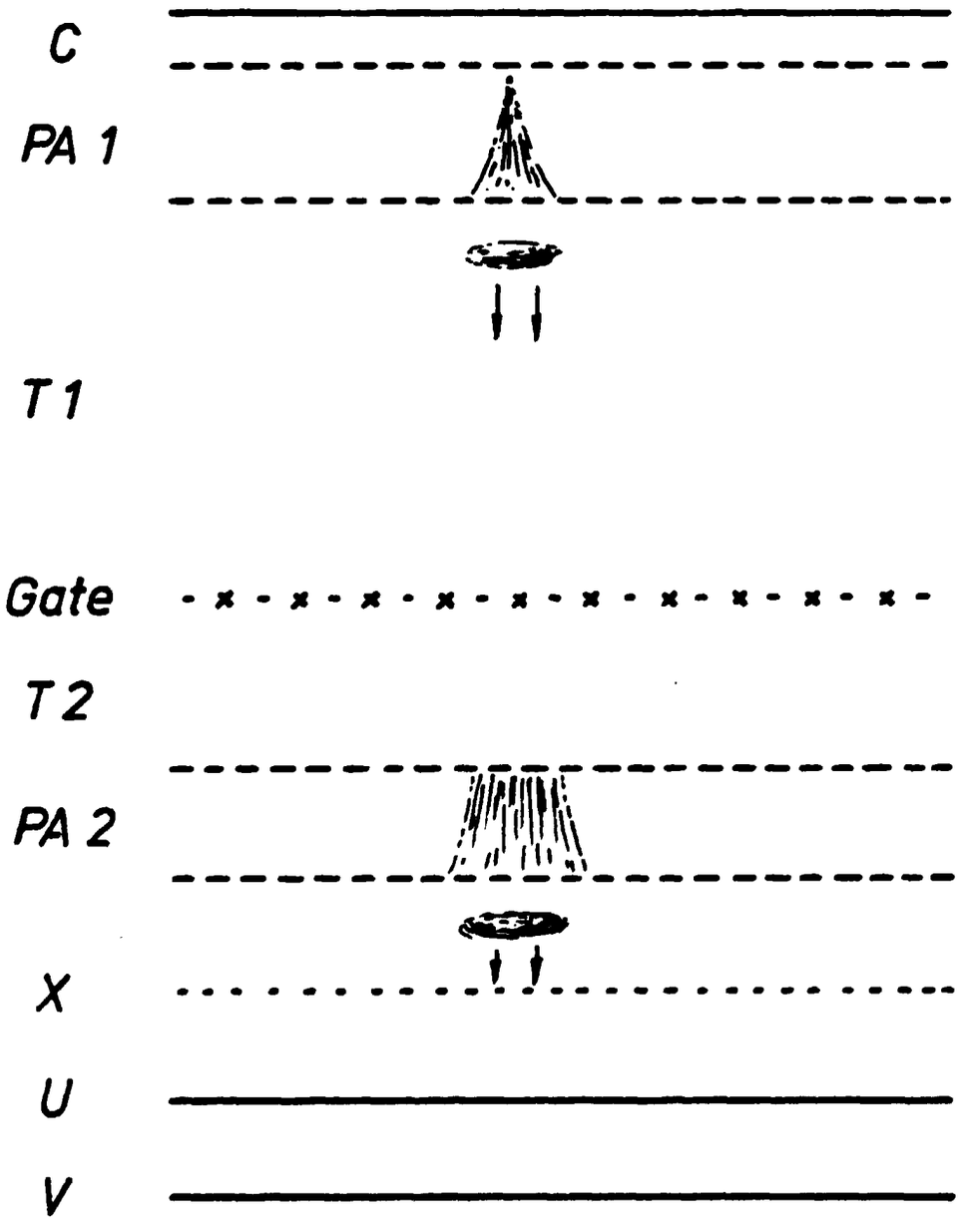

Fig : 4

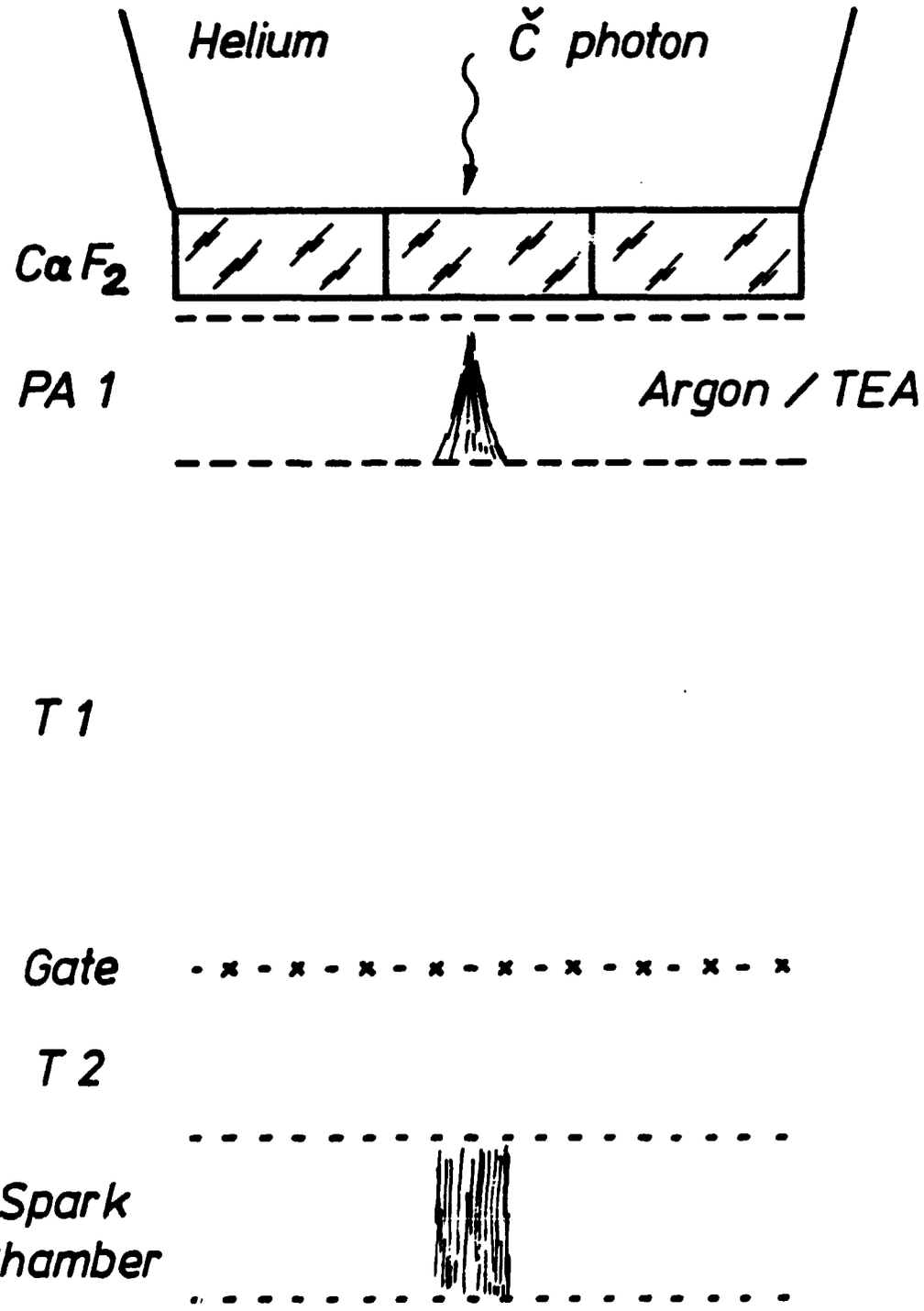

Fig: 5